

1 **Assessing the impact of Corona-virus-19 on nitrogen**
2 **dioxide levels over southern Ontario, Canada**

3 **Debora Griffin¹, Chris A. McLinden^{1,2}, Jacinthe Racine³, Michael D. Moran¹,**
4 **Vitali Fioletov¹, Radenko Pavlovic³, Henk Eskes⁴**

5 ¹Air Quality Research Division, Environment and Climate Change Canada, Toronto, Ontario, Canada

6 ²Institute of Space and Atmospheric Studies, University of Saskatchewan, Saskatoon, Saskatchewan,
7 Canada

8 ³Canadian Meteorological Centre Operations Division, Environment and Climate Change Canada, Dorval,
9 Quebec, Canada

10 ⁴Royal Netherlands Meteorological Institute (KNMI), De Bilt, The Netherlands

11 **Key Points:**

- 12 • Satellite NO₂ observations show a rapid decline following the COVID-19 associ-
13 ated lockdown and decrease by roughly 40% in Toronto.
14 • Meteorology is important when estimating emission reductions over a short time
15 period; in Toronto this accounts for about 20%.
16 • A lockdown emissions scenario with reductions in traffic, aviation, and industry
17 emissions represents the TROPOMI NO₂ observations well.

Corresponding author: Chris McLinden, chris.mclinden@canada.ca

Abstract

A lockdown was implemented in Canada mid-March 2020 to limit the spread of COVID-19. In the wake of this, declines in nitrogen dioxide (NO_2) were observed from the Tropospheric Monitoring Instrument (TROPOMI). A method is presented to quantify how much of this decrease is due to the lockdown itself as opposed to variability in meteorology and satellite sampling. The operational air quality forecast model, GEM-MACH, was used with TROPOMI to determine expected NO_2 columns that represents what TROPOMI would have observed for a non-COVID scenario. Decreases in NO_2 due to the lockdown were seen across southern Ontario, with an average 40% in Toronto and even larger declines in the city center. Natural and satellite sampling variability accounted for as much as 20–30%. A model run using a lockdown emissions scenario were found to be consistent with TROPOMI suggesting the prescribed declines in transportation and industry emissions are reasonable.

Plain Language Summary

States of emergency were declared throughout much of the world in the wake of the outbreak of Coronavirus disease in 2019 (COVID-19), with many countries, including Canada, imposing a lockdown. Consequently, emission patterns shifted away from transportation towards residential, leading overall to a sharp decrease observed levels of nitrogen dioxide (NO_2), an air pollutant which negatively impacts human and environmental health as seen from space-based sensors. Using satellite observations of NO_2 and air quality models, and accounting for confounding factors, we estimated that NO_2 levels in the Toronto, Canada area dropped by 40% during the lockdown and attribute this to reduced vehicle and aircraft traffic and reductions in industry.

1 Introduction

The outbreak of Coronavirus disease in late 2019 (COVID-19) reached Canada in early 2020, with the first Canadian COVID-related death reported in early March 2020. By mid-March provinces were beginning to limit the size of gatherings and initiating an overall lockdown of their populations. In Ontario, the lockdown was announced on March 16, 2020. This greatly disrupted traffic patterns, with traffic density observed to decrease by roughly 50% by early April. Travel restrictions also greatly curtailed air travel. These circumstances provided a unique and unprecedented natural experiment where emissions patterns were rapidly and drastically altered, especially in southern Ontario, home to the Greater Toronto Area (GTA), the most populous urban area in Canada. The GTA consists of the City of Toronto and four surrounding regional municipalities (see Supplement material Fig. S4) and includes many limited-access highways and expressways, rail lines, and Toronto Pearson International Airport, Canada's busiest airport. Its population in 2016 was over 6.4 million. Ultimately, the emissions changes in the GTA and the rest of southern Ontario associated with the pandemic will allow for testing and refining of emissions from different sectors, most notably those from vehicle traffic.

Nitrogen oxides ($\text{NO}_x = \text{NO}_2 + \text{NO}$) are primarily emitted during combustion processes and have adverse effects on human and environmental health: they are a key ingredient in smog, as precursors to both ozone and particulate matter, and can contribute to acid deposition. NO_x concentrations strongly correlate with local emission sources due to its short lifetime of a few hours (Valin et al., 2013; Beirle et al., 2011) and, because of the high and localized enhancements compared to background levels, NO_x is a good tracer of human activity near cities. For example, urban NO_x displays a strong weekly and diurnal cycle resulting from differences in traffic and manufacturing activity on weekends versus weekdays (Beirle et al., 2003; de Foy et al., 2016). Observed NO_2 is not merely a function of NO_x emissions; but is also a function of the local chemical environment and

67 meteorology. For example, it is well known that NO_2 impacts its own chemical lifetime
68 (Valin et al., 2013). Furthermore, meteorological parameters such as cloud cover, tem-
69 perature, and wind speed and direction all have a strong effect on local NO_2 enhance-
70 ments. Given this temporal and spatial variability in NO_2 , precisely where and when ob-
71 servations are made is also very important. Taken together, one important challenge when
72 interpreting changes in NO_2 lies in disentangling potential changes in emissions from nat-
73 ural and sampling variability.

74 Satellite observations can help to identify NO_x emissions and their variation glob-
75 ally. Declines of NO_2 emissions, following the lockdown, have previously been observed
76 by satellite instruments in China, India, Europe and North America (Zhang et al., 2020;
77 Bauwens et al., 2020; Shi & Brasseur, 2020). In this study, observations from the Eu-
78 ropean Space Agency’s Sentinel-5p Tropospheric Monitoring Instrument (TROPOMI),
79 in conjunction forecasts from Environment and Climate Change Canada’s (ECCC’s) op-
80 eration regional air quality forecast model GEM-MACH (Global Environmental Multi-
81 scale – Modelling Air quality and CHemistry) (Moran et al., 2010; Pendlebury et al., 2018),
82 are used to isolate the impact of the COVID associated lockdown on NO_2 levels in south-
83 ern Ontario, Canada. With the combination of satellite observations and model output
84 it is possible to determine the impact of meteorology and sampling variability on the ob-
85 served NO_2 column changes. The air quality model is further used to determine how pos-
86 sible lockdown-associated emission reductions impact the NO_2 columns, and whether those
87 match the observed changes.

88 2 Methodology

89 In the context of satellite remote sensing, one method, and the most straightfor-
90 ward, to assess the impact of the COVID lockdown on NO_2 is to directly compare the
91 COVID period with a non-COVID period, perhaps using the same period from differ-
92 ent years (Bauwens et al., 2020). However, in order to completely isolate the COVID sig-
93 nal, this method assumes that among the two periods being compared (i) baseline emis-
94 sions do not differ, (ii) natural or seasonal variability in winds, sunlight, temperature,
95 and other meteorological parameters are not important, (iii) differences in satellite sam-
96 pling do not play any role, and (iv) any differences in the satellite retrieval algorithm are
97 minimal. For many locations, including the Canadian domain studied here, differences
98 in interannual NO_x emission changes should be small, but meteorological variability can
99 be important, and given that, sampling variability is also likely to lead to differences in
100 the two periods. In the case of TROPOMI, different retrieval algorithms were used for
101 spring 2019 vs. spring 2020 (v1.2 until April 2019 and thereafter v1.3, differences include
102 the treatment of “negative” cloud fractions and the lower limit of the tropospheric air
103 mass factor (AMF) relaxed influencing the qa_value). While differences tend to be small,
104 it is difficult at present to completely eliminate this as a possible source of difference.

105 With these confounding factors in mind, the method used here is one in which the
106 ECCC’s operational GEM-MACH air quality model forecasts are used to control for non-
107 COVID factors such as sampling variability, meteorological variability, and other sources
108 of variability. Furthermore, to limit potential differences in the retrieval algorithm be-
109 tween 2019 and 2020, the two periods considered are consecutive in 2020: a pre-COVID
110 period and the COVID-lockdown period.

111 2.1 TROPOMI Observations

112 Observations of NO_2 from the European Space Agency Tropospheric Monitoring
113 Instrument (TROPOMI, 2017-present; Veefkind et al. (2012)), an Earth-viewing spec-
114 trometer, are used here. TROPOMI has a resolution of $3.5 \times 5.5 \text{ km}^2$ (since August 2019,
115 before $3.5 \times 7 \text{ km}^2$) at nadir and measures back-scattered UV/visible/solar-IR sunlight
116 from which NO_2 vertical column density (VCD), or the vertically-integrated NO_2 num-

117 ber density, can be derived. Details on the retrieval algorithm can be found elsewhere
118 (van Geffen et al., 2019), but in short: a spectral fit is performed matching laboratory-
119 measured NO_2 absorption cross-sections and other relevant parameters to these observed
120 spectra which provide a determination of the NO_2 slant column densities (SCDs), or the
121 number density integrated along the path of the sunlight through the atmosphere. In
122 a second step, the stratospheric component of the SCD is determined using a chemical
123 data assimilated system and subtracted. Finally, the remaining tropospheric SCD was
124 then converted to a VCD using an AMF which quantifies the sensitivity of the satellite
125 to a particular scene which depends on factors such as shape of the NO_2 profile and sur-
126 face reflectivity. In this work, an alternative air mass factor is used which better accounts
127 for the presence of snow and uses higher resolution NO_2 profile shapes to improve the
128 effective spatial resolution (McLinden et al., 2014; Griffin et al., 2019); see Supplement
129 material for more information (Côté et al., 1998; Girard et al., 2014; Houyoux et al., 2000;
130 Schaaf et al., 2002; Makar, Gong, Milbrandt, et al., 2015; Makar, Gong, Hogrefe, et al.,
131 2015; Gong et al., 2015, 2018; Akingunola et al., 2018; Cooper et al., 2018). A radiative
132 transfer model is used to calculate AMFs (Palmer et al., 2001) which depends on fac-
133 tors such as solar and viewing geometry, the presence of clouds, scene reflectivity and
134 the vertical distribution of the NO_2 via $\text{VCD}=\text{SCD}/\text{AMF}$. Lastly, the TROPOMI data
135 are filtered to use only the highest quality data ($\text{qa_value}> 0.75$ and the cloud cover of
136 the pixels is at most 30%).

137 2.2 GEM-MACH Air Quality Forecast Model

138 The Canadian operational air quality forecast model, GEM-MACH (Moran et al.,
139 2010; Pavlovic et al., 2016; Makar et al., 2017; Pendlebury et al., 2018), is used in this
140 work. GEM-MACH consists of an on-line chemical transport module that is embedded
141 within ECCO’s Global Environmental Multi-scale (GEM), weather forecast model, and
142 is applied over a domain that covers most of North America. It includes emissions, chem-
143 istry, dispersion, and removal process representations for 41 gaseous and eight particle
144 chemical species, and provides hourly concentrations between the surface and 0.1 Pa (on
145 80 hybrid vertical levels) with a $10\times 10\text{ km}^2$ grid cell. The standard operational model
146 run inputs hourly emissions fields that are prepared using the Sparse Matrix Operator
147 Kernel Emissions (SMOKE) (Coats, 1996) that account for seasonal, weekly and daily
148 variations. The current version of the emissions files used by the operational model are
149 based on a Canadian emissions inventory compiled for the 2013 base year and a 2017 pro-
150 jected U.S. inventory (Moran & Ménard, 2019). While using year-specific NO_x emissions
151 is ideal, suitable emission inventories are not available in a timely manner. Alternative
152 non-operational runs were also performed for a limited time period between March 15
153 and May 10, 2020 with updated Canadian base-year emissions and COVID-modified emis-
154 sions for vehicle, aircraft, manufacturing, and residential sectors (see Sect. 3 for details)

155 .
156 GEM-MACH output is used in this study for two purposes. The first is to provide
157 profile shapes which are used in the calculation of revised TROPOMI AMFs as discussed
158 above in section 2.1. The second is to determine the time evolution of NO_2 on standard
159 ”business as usual” (BAU) input emissions that do not account for COVID impacts, which
160 can then be contrasted with that observed by TROPOMI. In both cases, NO_2 profiles
161 are obtained from operational forecasts, run at 10 km spatial resolution and launched
162 every 12 hours (and every 24 hours for the special runs).

163 In this study, we integrate the model NO_2 profiles to obtain VCD values. The op-
164 erational GEM-MACH model currently does not include NO_x sources in the free tropo-
165 sphere (such as lightning and aircraft at cruising altitude); as a consequence the model
166 NO_x concentrations are near zero above the boundary layer. We obtain a more realis-
167 tic free tropospheric column from a monthly GEOS-Chem run (averaged between 18-
168 21 UTC, from 2 km to 12 km; $0.5\times 0.67^\circ$ resolution, version v8-03-01; <http://www.geos->

169 chem.org; Bey et al. (2001)), these partial columns are on the order of 10^{14} molec/cm².
 170 The model VCDs are then sampled (and filtered) in space and time at each TROPOMI
 171 pixel, and filtered like the TROPOMI observations.

172 2.3 Determination of Expected NO₂

173 In order to estimate the impact of the COVID measures on NO₂ levels, isolated
 174 from any other possible sources of variability, including seasonal, inter-annual, or shorter-
 175 term meteorological variability, and TROPOMI sampling variability, GEM-MACH out-
 176 put is used. GEM-MACH forecasts using standard emissions inventories for both the pre-
 177 lockdown and lockdown periods, are sampled at each TROPOMI pixel and overpass time.

178 Comparing pre-lockdown and lockdown TROPOMI observations together with pre-
 179 lockdown and lockdown GEM-MACH predictions will provide an estimate of the changes
 180 in NO_x emissions purely due to the lockdown, as this method accounts for effects of me-
 181 teorology, seasonality, and sampling variability. The expected TROPOMI VCDs, $V_{T,e}$,
 182 under a BAU scenario, are determined from the TROPOMI VCDs before the lockdown
 183 and adjusted by the relative change seen in the model forecasts (GEM-MACH and free
 184 troposphere from GEOS-Chem) between the two time periods:

$$V_{T,e}(t_{covid}) = V_T(t_{pre}) \cdot \frac{V_{Model}(t_{covid})}{V_{Model}(t_{pre})}. \quad (1)$$

185 When averaging over time to produce spatially resolved maps, observations from Febru-
 186 ary 15 to March 15, 2020 and March 16 to May 8, 2020 are used for the pre-lockdown
 187 and lockdown time periods, respectively. This end date is associated with some traffic
 188 rebound and increased emissions throughout May 2020 (see Sect. 3). When averaging
 189 spatially over an area to produce a time series, 15-day running means are used (the satel-
 190 lite data need to be averaged over multiple days in order to obtain enough data over this
 191 area, approximately 50 % of observations are filtered due to clouds). The expected columns
 192 for the 15-day running means are estimated as in Eq. 1, where $V_{T,e}(t_{covid})$ and $V_{Model}(t_{covid})$
 193 are the 15-day means for a specific day.

194 3 Results

195 Figure 1 shows the TROPOMI and operational GEM-MACH NO₂ VCDs averaged
 196 over the pre-lockdown and lockdown periods. There is excellent agreement between TROPOMI,
 197 panel (a), and GEM-MACH, panel (d), across southern Ontario for the pre-lockdown
 198 period in terms of both spatial distribution and magnitudes which provides confidence
 199 that the NO_x emissions inventory and the model itself can accurately represent the com-
 200 plex physics and photochemistry of the real world.

201 When comparing TROPOMI observations between the pre-lockdown and lockdown
 202 periods, panel (a)–(c), there is a large decrease in VCDs over the GTA, the Windsor-
 203 Detroit urban area (which straddles the Canada-U.S. border), and virtually the entire
 204 domain. Decreases in the urban areas can reach or exceed 50%, and in parts of the GTA
 205 the decline can even exceed 60 %. However, there is also a decrease predicted by GEM-
 206 MACH, despite not accounting for COVID-related emissions reductions as shown in pan-
 207 els (d)–(f). This is due to a combination of a seasonal effect in which increased sunlight
 208 means a decrease in NO_x lifetime and less NO_x present as NO₂, but also expected sea-
 209 sonal changes in emissions (see Supplement material Fig. S2). This effect is on the or-
 210 der of 25 % over the GTA between the two time periods, and is especially large because
 211 it occurs during the change from cold season to warm season.

212 Even using several weeks of TROPOMI observations, meteorological and sampling
 213 variability can impact the average. Spring 2020 was colder than 2019 and particularly
 214 cloudy over southern Ontario, leading to fewer cloud-free overpasses on which to base

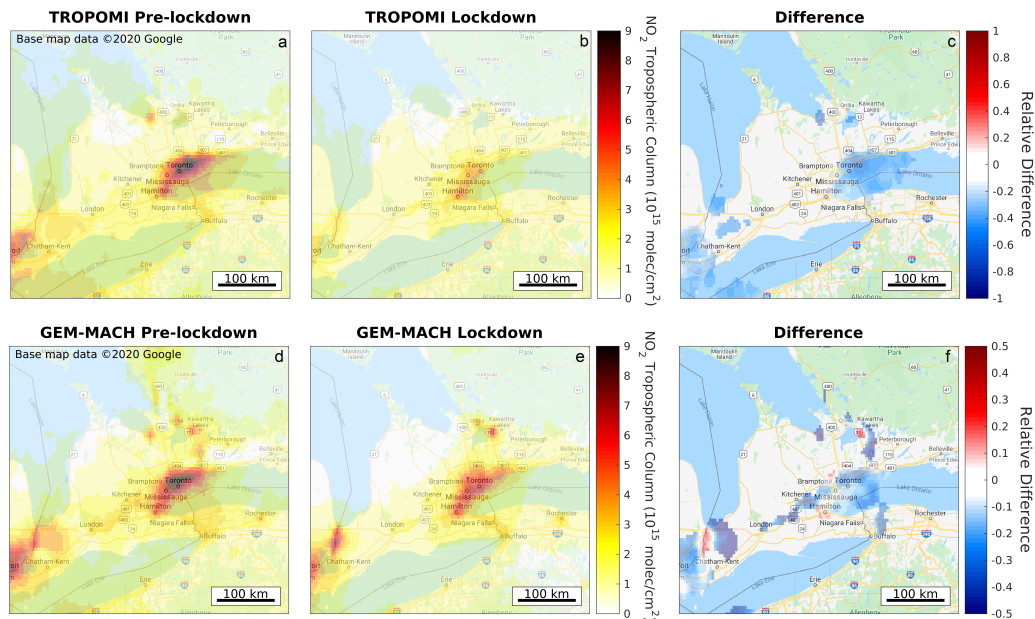


Figure 1. TROPOMI averaged VCDs over southern Ontario are shown for (a) a pre-lockdown (16 February – 15 March 2020; top) and (b) a lockdown (16 March – 8 May 2020) period. The relative differences are shown in panel (c) for areas that exceed 3×10^{15} molec/cm² in the pre-lockdown period. Panels (d), (e), (f) are the same but for the operational GEM-MACH model BAU NO₂ VCDs, sampled at the time and location of the TROPOMI pixels.

215 an average. The impact of the TROPOMI sampling pattern was investigated (see Sup-
 216 plement material Fig. S1). In general, approximately 50 % of TROPOMI data were re-
 217 moved due to cloud cover, so that the remaining cloud-free observations will be more rep-
 218 resentative of fair weather conditions. To determine the impact of the sampling variabil-
 219 ity, GEM-MACH averages were determined using all days over the entire domain, ver-
 220 sus only those sampled as TROPOMI ($qa > 0.75$). For the average NO₂ between March
 221 16 and May 8, 2020, sampling variability can lead to differences as large as 10 % near
 222 cities.

223 As a test of the methodology to create expected TROPOMI columns for the COVID-
 224 19 period from the change in the model forecasts, the same procedure was applied to TROPOMI
 225 observations and operational GEM-MACH output from 2019. In this case, differences
 226 between expected and TROPOMI observations should be minimal. As can be seen in
 227 Figs. 2d and 2e, differences are small, suggesting the method is generally reliable. Av-
 228 eraged over the GTA, differences are 0–2%.

229 To help evaluate the difference between expected and observed TROPOMI NO₂
 230 columns, as shown in Fig. 2, GEM-MACH was re-run using an alternative emissions sce-
 231 nario designed to represent COVID-19 emissions changes: (i) a 30 % reduction in indus-
 232 trial NO_x emissions, (ii) a 60 % reduction for traffic NO_x emissions, (iii) an 80 % re-
 233 duction in aircraft NO_x emissions (landings and takeoffs), and (iv) a 20 % increase of res-
 234 idential fuel NO_x emissions due to people staying at home. Emissions of other air pol-
 235 lutants emitted by these source types (CO, VOC, NH₃, SO₂, PM_{2.5}, PM₁₀) were also
 236 changed by these same percentages. This scenario was determined using expert engineer-
 237 ing judgement and, in the case of traffic emissions, is supported by observed changes in
 238 traffic counts. Over the entire GTA, average emissions went from 65 kt[NO₂]/yr pre-lockdown

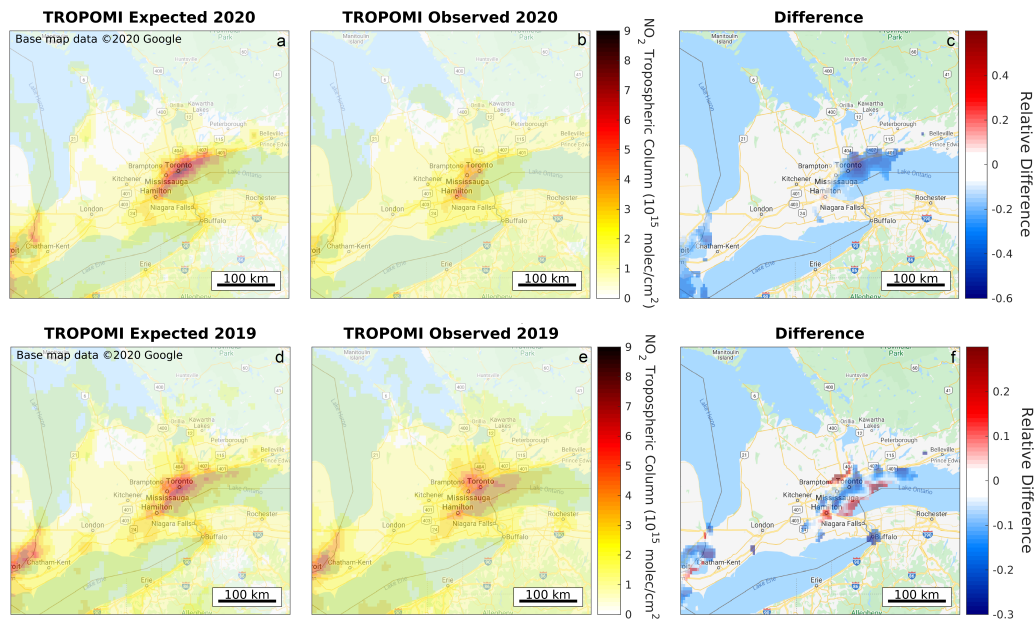


Figure 2. Expected and observed TROPOMI average VCD fields over southern Ontario for the lockdown period (16 March – 8 May 2020) are shown in panels (a) and (b), respectively. The same is shown in panels (d) and (e), but for 16 March – 8 May, 2019. Relative differences (for areas that exceed 3×10^{15} molec/cm²) between the TROPOMI observations and the expected columns are shown in panel (c) and (f) for 2020 and 2019, respectively. Note that panel (b) is the same as Figure 1b.

239 to 40 kt[NO₂]/yr lockdown (around noon; see Figs. S3, S5 and S6). Note that only Cana-
 240 dian emissions were adjusted in this way due to the challenge of representing the comp-
 241 plicated mixture of city-, county-, and state-level responses to COVID-19 in the U.S.,
 242 but given the short atmospheric lifetime of NO_x this is unlikely to make a big difference
 243 to NO₂ levels except close to the international border. The results of this emissions sce-
 244 nario run are shown and compared to TROPOMI observations in Figs. 3 (for 1 April
 245 to May 8, 2020). Good agreement is evident over much of southern Ontario.

246 An alternative method of considering these various data sources is to average spa-
 247 tially and look at temporal changes. Figure 4 shows a time series of 15-day running av-
 248 erage NO₂ over the Toronto and Mississauga area (part of the GTA with the highest emis-
 249 sions and population density, this area also includes Toronto Pearson Airport; see Sup-
 250 plement material Fig. S4). TROPOMI observations show a decline after the lockdown
 251 was announced (Fig. 4a), the expected columns agree well with the TROPOMI obser-
 252 vations during the pre-lockdown period, but, differences emerge after the lockdown be-
 253 gins as emissions are reduced, but the model assumes BAU emissions. The alternate model
 254 run with reduced emissions (Fig. 4b) represents the decline observed by TROPOMI quite
 255 well and over the same time period, both the TROPOMI observations and the model
 256 predict a drop of roughly 40% over the GTA core (using data from March 16 to May
 257 8, 2020) as a result of the lockdown. When the 2019 and 2020 satellite data are com-
 258 pared directly, however, the drop is only about half as much (20%), as the meteorology
 259 and sampling variability of the satellite were largely different in that area between
 260 2019 and 2020. Note that the satellite data indicate that the peak of the emissions decline
 261 in Toronto and Mississauga occurred in mid-April. Throughout May 2020, the satellite
 262 measurements suggest that the NO_x emissions began to increase again gradually (Fig. 4a),

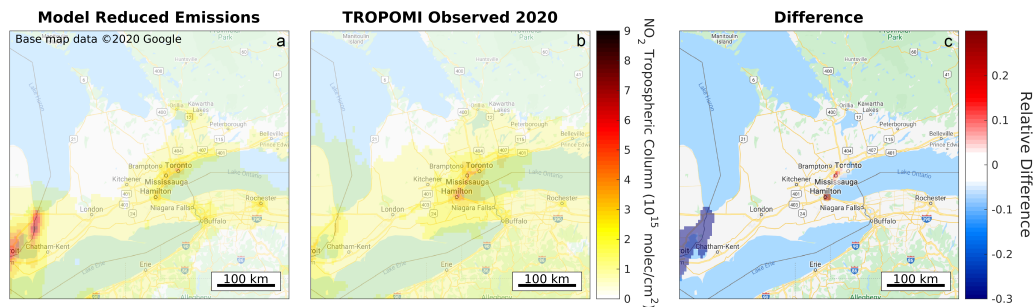


Figure 3. Model NO_2 VCDs from the reduced emissions scenario (a) and observed TROPOMI NO_2 VCDs (b) over southern Ontario averaged over the period 1 April – 8 May 2020. The relative differences are shown in panel (c) for areas that exceed 3×10^{15} molec/cm². Note that emissions have only been reduced in Canada; thus, large differences can be seen for the US cities near the border, especially Detroit.

263 though they are still lower than BAU emissions. Ontario entered Phase 1 of its re-opening
 264 on May 19, 2020, when certain restrictions were lifted.

265 4 Summary

266 We present a method to entangle the effects of meteorology and sampling variability
 267 on the observed NO_2 changes, from the lockdown-related changes in NO_x emissions.
 268 During the period from March 16 to May 8 2020, NO_2 columns in the center of the GTA
 269 decreased by nearly 60% compared to the previous month. About 25% of this decrease
 270 is associated with meteorological and seasonal changes independent of the COVID-19
 271 pandemic. Even the TROPOMI sampling variability itself can impact the magnitude of
 272 the observed NO_2 columns over the course of one or two months averaging ($\sim 10\%$). From
 273 the TROPOMI observations and GEM-MACH air quality model results, we estimate that
 274 due to the lockdown the NO_2 columns in Toronto and Mississauga declined by over 40%.
 275 These changes vary spatially, and in certain locations columns declined by over 50%. Re-
 276 ducing the NO_x input emissions of vehicle traffic, aircraft, and industry used by the GEM-
 277 MACH model resulted in a similar pattern as observed by TROPOMI, resulting in a drop
 278 of 36% in NO_2 columns over the Mississauga and Toronto area. Although, spatial pat-
 279 terns over cities are somewhat visible, it is hard to disentangle the emission reductions
 280 by sector with our methodology. Nevertheless, emission changes of (i) a 30% reduction
 281 in industry, (ii) a 60% reduction for traffic, (iii) an 80% reduction in aircraft landings
 282 and takeoffs, and (iv) a 20% increase in residential fuel combustion, represent the TROPOMI
 283 NO_2 observations well, at least in southern Ontario. In the GTA, NO_x emissions of 40
 284 kt[NO_2]/yr represent the observations well, this is a drop of over 37% compared to a busi-
 285 ness as usual scenario. The drop in the input emissions is almost identical to the drop
 286 determined from the model NO_2 VCDs (36%) over the same area which further indi-
 287 cates that the method presented works well.

288 This study highlights the importance of considering meteorological and sampling
 289 variability when estimating emission reductions. One needs to be cautious when simply
 290 comparing two months, since the effects of meteorological and sampling variability are
 291 not negligible when only a short series of data is averaged. As well, the emissions may
 292 vary strongly spatially, especially in cities. This can make it difficult to compare differ-
 293 ent studies unless the exact same areas are considered. The unique lockdown period as-
 294 sociated with the 2020 COVID-19 pandemic can further be used to check and refine our
 295 existing emissions inventories for NO_x and other pollutants by looking at spatial and tem-

296 poral distributions of available satellite and surface measurements for a number of dif-
 297 ferent urban areas.

298 Acknowledgments

299 This work contains modified Copernicus Sentinel data. The Sentinel 5 Precursor TROPOMI
 300 Level 2 product is developed with funding from the Netherlands Space Office (NSO) and
 301 processed with funding from the European Space Agency (ESA). TROPOMI data can
 302 be downloaded from <https://s5phub.copernicus.eu> (last access: June 16, 2020). We would
 303 like to thank you MSC-REQA employees involved in emission adjustment and modelling:
 304 Rabab Mashayekhi, Mourad Sassi, Annie Duhamel and Jessica Miville.

305 References

- 306 Akingunola, A., Makar, P. A., Zhang, J., Darlington, A., Li, S.-M., Gordon, M.,
 307 ... Zheng, Q. (2018). A chemical transport model study of plume-rise
 308 and particle size distribution for the Athabasca oil sands. *Atmospheric*
 309 *Chemistry and Physics*, 18(12), 8667–8688. Retrieved from [https://](https://www.atmos-chem-phys.net/18/8667/2018/)
 310 www.atmos-chem-phys.net/18/8667/2018/ doi: 10.5194/acp-18-8667-2018
- 311 Bauwens, M., Compernelle, S., Stavrakou, T., Müller, J.-F., van Gent, J., Es-
 312 kes, H., ... Zehner, C. (2020). Impact of coronavirus outbreak on NO₂
 313 pollution assessed using TROPOMI and OMI observations. *Geophysical*
 314 *Research Letters*, n/a(n/a), e2020GL087978. Retrieved from [https://](https://agupubs.onlinelibrary.wiley.com/doi/abs/10.1029/2020GL087978)
 315 agupubs.onlinelibrary.wiley.com/doi/abs/10.1029/2020GL087978
 316 (e2020GL087978 2020GL087978) doi: 10.1029/2020GL087978
- 317 Beirle, S., Boersma, K. F., Platt, U., Lawrence, M. G., & Wagner, T. (2011). Megac-
 318 ity emissions and lifetimes of nitrogen oxides probed from space. *Science*,
 319 333(6050), 1737–1739. Retrieved from [http://science.sciencemag.org/](http://science.sciencemag.org/content/333/6050/1737)
 320 [content/333/6050/1737](http://science.sciencemag.org/content/333/6050/1737) doi: 10.1126/science.1207824
- 321 Beirle, S., Platt, U., Wenig, M., & Wagner, T. (2003). Weekly cycle of NO₂
 322 by GOME measurements: a signature of anthropogenic sources. *Atmo-*
 323 *spheric Chemistry and Physics*, 3(6), 2225–2232. Retrieved from [https://](https://www.atmos-chem-phys.net/3/2225/2003/)
 324 www.atmos-chem-phys.net/3/2225/2003/ doi: 10.5194/acp-3-2225-2003
- 325 Bey, I., Jacob, D. J., Yantosca, R. M., Logan, J. A., Field, B. D., Fiore, A. M., ...
 326 Schultz, M. G. (2001). Global modeling of tropospheric chemistry with assim-
 327 ilated meteorology: Model description and evaluation. *Journal of Geophysical*
 328 *Research: Atmospheres*, 106(D19), 23073–23095. Retrieved from [https://](https://agupubs.onlinelibrary.wiley.com/doi/abs/10.1029/2001JD000807)
 329 agupubs.onlinelibrary.wiley.com/doi/abs/10.1029/2001JD000807 doi:
 330 10.1029/2001JD000807
- 331 Coats, C. J. (1996). High-performance algorithms in the sparse matrix operator
 332 kernel emissions (SMOKE) modeling system. Atlanta, GA, USA: American
 333 Meteorological Society. (Proceedings of the Ninth AMS Joint Conference on
 334 Applications of Air Pollution Meteorology with AWMA, 28 January–2 Febru-
 335 ary 1996)
- 336 Cooper, M. J., Martin, R. V., Lyapustin, A. I., & McLinden, C. A. (2018). Assess-
 337 ing snow extent data sets over North America to inform and improve trace gas
 338 retrievals from solar backscatter. *Atmospheric Measurement Techniques*, 11(5),
 339 2983–2994. Retrieved from [https://www.atmos-meas-tech.net/11/2983/](https://www.atmos-meas-tech.net/11/2983/2018/)
 340 [2018/](https://www.atmos-meas-tech.net/11/2983/2018/) doi: 10.5194/amt-11-2983-2018
- 341 Côté, J., Gravel, S., Méthot, A., Patoine, A., Roch, M., & Staniforth, A. (1998).
 342 The Operational CMC–MRB Global Environmental Multiscale (GEM)
 343 Model. Part I: Design Considerations and Formulation. *Monthly Weather*
 344 *Review*, 126(6), 1373–1395. Retrieved from [https://doi.org/10.1175/](https://doi.org/10.1175/1520-0493(1998)126<1373:TOCMGE>2.0.CO;2)
 345 [1520-0493\(1998\)126<1373:TOCMGE>2.0.CO;2](https://doi.org/10.1175/1520-0493(1998)126<1373:TOCMGE>2.0.CO;2) doi: 10.1175/1520-0493(1998)
 346 126(1373:TOCMGE)2.0.CO;2

- 347 de Foy, B., Lu, Z., & Streets, D. G. (2016). Satellite NO₂ retrievals suggest China
 348 has exceeded its NO_x reduction goals from the twelfth Five-Year Plan. *Sci-*
 349 *entific Reports*, 6(35912). Retrieved from [http://dx.doi.org/10.1038/](http://dx.doi.org/10.1038/srep35912)
 350 [srep35912](http://dx.doi.org/10.1038/srep35912) doi: 10.1038/srep35912
- 351 Girard, C., Plante, A., Desgagné, M., McTaggart-Cowan, R., Côté, J., Charron,
 352 M., ... Zadra, A. (2014). Staggered Vertical Discretization of the Cana-
 353 dian Environmental Multiscale (GEM) Model Using a Coordinate of the
 354 Log-Hydrostatic-Pressure Type. *Monthly Weather Review*, 142(3), 1183-
 355 1196. Retrieved from <https://doi.org/10.1175/MWR-D-13-00255.1> doi:
 356 10.1175/MWR-D-13-00255.1
- 357 Gong, W., Beagley, S. R., Cousineau, S., Sassi, M., Munoz-Alpizar, R., Ménard,
 358 S., ... Holt, R. (2018). Assessing the impact of shipping emissions on air
 359 pollution in the Canadian Arctic and northern regions: current and future
 360 modelled scenarios. *Atmospheric Chemistry and Physics*, 18(22), 16653–16687.
 361 Retrieved from <https://www.atmos-chem-phys.net/18/16653/2018/> doi:
 362 10.5194/acp-18-16653-2018
- 363 Gong, W., Makar, P., Zhang, J., Milbrandt, J., Gravel, S., Hayden, K., ... Leitch,
 364 W. (2015). Modelling aerosol–cloud–meteorology interaction: A case study
 365 with a fully coupled air quality model (GEM-MACH). *Atmospheric Envi-*
 366 *ronment*, 115, 695 - 715. Retrieved from [http://www.sciencedirect.com/](http://www.sciencedirect.com/science/article/pii/S1352231015301333)
 367 [science/article/pii/S1352231015301333](http://www.sciencedirect.com/science/article/pii/S1352231015301333) doi: [https://doi.org/10.1016/](https://doi.org/10.1016/j.atmosenv.2015.05.062)
 368 [j.atmosenv.2015.05.062](https://doi.org/10.1016/j.atmosenv.2015.05.062)
- 369 Griffin, D., Zhao, X., McLinden, C. A., Boersma, F., Bourassa, A., Dammers, E.,
 370 ... Wolde, M. (2019). High-Resolution Mapping of Nitrogen Dioxide With
 371 TROPOMI: First Results and Validation Over the Canadian Oil Sands.
 372 *Geophysical Research Letters*, 46(2), 1049-1060. Retrieved from [https://](https://agupubs.onlinelibrary.wiley.com/doi/abs/10.1029/2018GL081095)
 373 agupubs.onlinelibrary.wiley.com/doi/abs/10.1029/2018GL081095 doi:
 374 10.1029/2018GL081095
- 375 Houyoux, M. R., Vukovich, J. M., Coats Jr., C. J., Wheeler, N. J. M., & Kasibhatla,
 376 P. S. (2000). Emission inventory development and processing for the Seasonal
 377 Model for Regional Air Quality (SMRAQ) project. *Journal of Geophysi-*
 378 *cal Research: Atmospheres*, 105(D7), 9079-9090. Retrieved from [https://](https://agupubs.onlinelibrary.wiley.com/doi/abs/10.1029/1999JD900975)
 379 agupubs.onlinelibrary.wiley.com/doi/abs/10.1029/1999JD900975 doi:
 380 10.1029/1999JD900975
- 381 Makar, P. A., Gong, W., Hogrefe, C., Zhang, Y., Curci, G., Žabkar, R., ... Gal-
 382 marini, S. (2015). Feedbacks between air pollution and weather, part 2: Effects
 383 on chemistry. *Atmospheric Environment*, 115, 499 – 526. Retrieved from
 384 <http://www.sciencedirect.com/science/article/pii/S1352231014008103>
 385 doi: <https://doi.org/10.1016/j.atmosenv.2014.10.021>
- 386 Makar, P. A., Gong, W., Milbrandt, J., Hogrefe, C., Zhang, Y., Curci, G., ... Gal-
 387 marini, S. (2015, 08). Feedbacks between air pollution and weather, Part 1:
 388 Effects on weather. *Atmospheric Environment*, 115.
- 389 Makar, P. A., Staebler, R. M., Akingunola, A., Zhang, J., McLinden, C., Kharol,
 390 S. K., ... Zheng, Q. (2017). The effects of forest canopy shading and
 391 turbulence on boundary layer ozone. *Nature Communications*, 8. doi:
 392 10.1038/ncomms15243
- 393 McLinden, C. A., Fioletov, V., Boersma, K. F., Kharol, S. K., Krotkov, N., Lam-
 394 sal, L., ... Yang, K. (2014). Improved satellite retrievals of NO₂ and
 395 SO₂ over the Canadian oil sands and comparisons with surface measure-
 396 ments. *Atmospheric Chemistry and Physics*, 14(7), 3637–3656. Re-
 397 trieved from <https://www.atmos-chem-phys.net/14/3637/2014/> doi:
 398 10.5194/acp-14-3637-2014
- 399 Moran, M. D., & Ménard, S. (2019). Regional Air Quality Deter-
 400 ministic Prediction System (RAQDPS): Update from version 020.2
 401 to version 021. Montreal, CA: Canadian Centre for Meteorolog-

- ical and Environmental Prediction. (Technical note, p. 49 pp.,
http://collaboration.cmc.ec.gc.ca/cmc/cmci/product_guide/docs/tech_notes/technote_raqdps-021_20190703.e.pdf [last access: 23 June 2020])
- Moran, M. D., Ménard, S., Talbot, D., Huang, P., Makar, P. A., Gong, W., ... Sassi, M. (2010). *Particulate-matter forecasting with GEM-MACH15, a new Canadian air-quality forecast model*, in: *Air Pollution Modelling and Its Application XX*. Dordrecht, the Netherlands: Springer.
- Palmer, P. I., Jacob, D. J., Chance, K., Martin, R. V., Spurr, R. J. D., Kurosu, T. P., ... Li, Q. (2001). Air mass factor formulation for spectroscopic measurements from satellites: Application to formaldehyde retrievals from the Global Ozone Monitoring Experiment. *Journal of Geophysical Research: Atmospheres*, 106(D13), 14539-14550. Retrieved from <https://agupubs.onlinelibrary.wiley.com/doi/abs/10.1029/2000JD900772> doi: 10.1029/2000JD900772
- Pavlovic, R., Chen, J., Anderson, K., Moran, M. D., Beaulieu, P.-A., Davignon, D., & Cousineau, S. (2016). The FireWork air quality forecast system with near-real-time biomass burning emissions: Recent developments and evaluation of performance for the 2015 North American wildfire season. *Journal of the Air & Waste Management Association*, 66(9), 819-841. Retrieved from <https://doi.org/10.1080/10962247.2016.1158214> (PMID: 26934496) doi: 10.1080/10962247.2016.1158214
- Pendlebury, D., Gravel, S., Moran, M. D., & Lupu, A. (2018). Impact of chemical lateral boundary conditions in a regional air quality forecast model on surface ozone predictions during stratospheric intrusions. *Atmospheric Environment*, 174, 148 - 170. Retrieved from <http://www.sciencedirect.com/science/article/pii/S1352231017307185> doi: <https://doi.org/10.1016/j.atmosenv.2017.10.052>
- Schaaf, C. B., Gao, F., Strahler, A. H., Lucht, W., Li, X., Tsang, T., ... Roy, D. (2002). First operational brdf, albedo nadir reflectance products from modis. *Remote Sensing of Environment*, 83(1), 135 - 148. Retrieved from <http://www.sciencedirect.com/science/article/pii/S0034425702000913> (The Moderate Resolution Imaging Spectroradiometer (MODIS): a new generation of Land Surface Monitoring) doi: [https://doi.org/10.1016/S0034-4257\(02\)00091-3](https://doi.org/10.1016/S0034-4257(02)00091-3)
- Shi, X., & Brasseur, G. P. (2020). The Response in Air Quality to the Reduction of Chinese Economic Activities during the COVID-19 Outbreak. *Geophysical Research Letters*, n/a(n/a), e2020GL088070. Retrieved from <https://agupubs.onlinelibrary.wiley.com/doi/abs/10.1029/2020GL088070> (e2020GL088070 2020GL088070) doi: 10.1029/2020GL088070
- Valin, L. C., Russell, A. R., & Cohen, R. C. (2013). Variations of OH radical in an urban plume inferred from NO₂ column measurements. *Geophysical Research Letters*, 40(9), 1856-1860. Retrieved from <http://dx.doi.org/10.1002/grl.50267> doi: 10.1002/grl.50267
- van Geffen, J., Boersma, K. F., Eskes, H., Sneep, M., ter Linden, M., Zara, M., & Veefkind, J. P. (2019). S5P/TROPOMI NO₂ slant column retrieval: method, stability, uncertainties, and comparisons against OMI. *Atmospheric Measurement Techniques Discussions*, 2019, 1-33. Retrieved from <https://www.atmos-meas-tech-discuss.net/amt-2019-471/> doi: 10.5194/amt-2019-471
- Veefkind, J., Aben, I., McMullan, K., Forster, H., de Vries, J., Otter, G., ... Levelt, P. (2012). TROPOMI on the ESA Sentinel-5 Precursor: A GMES mission for global observations of the atmospheric composition for climate, air quality and ozone layer applications. *Remote Sensing of Environment*, 120, 70 - 83. Retrieved from <http://www.sciencedirect.com/science/article/pii/S0034425712000661> (The Sentinel Missions - New Opportunities for Science)

457 doi: <https://doi.org/10.1016/j.rse.2011.09.027>
458 Zhang, R., Zhang, Y., Lin, H., Feng, X., Fu, T.-M., & Wang, Y. (2020). NO_x Emis-
459 sion Reduction and Recovery during COVID-19 in East China. *Atmosphere*,
460 *11*(433).

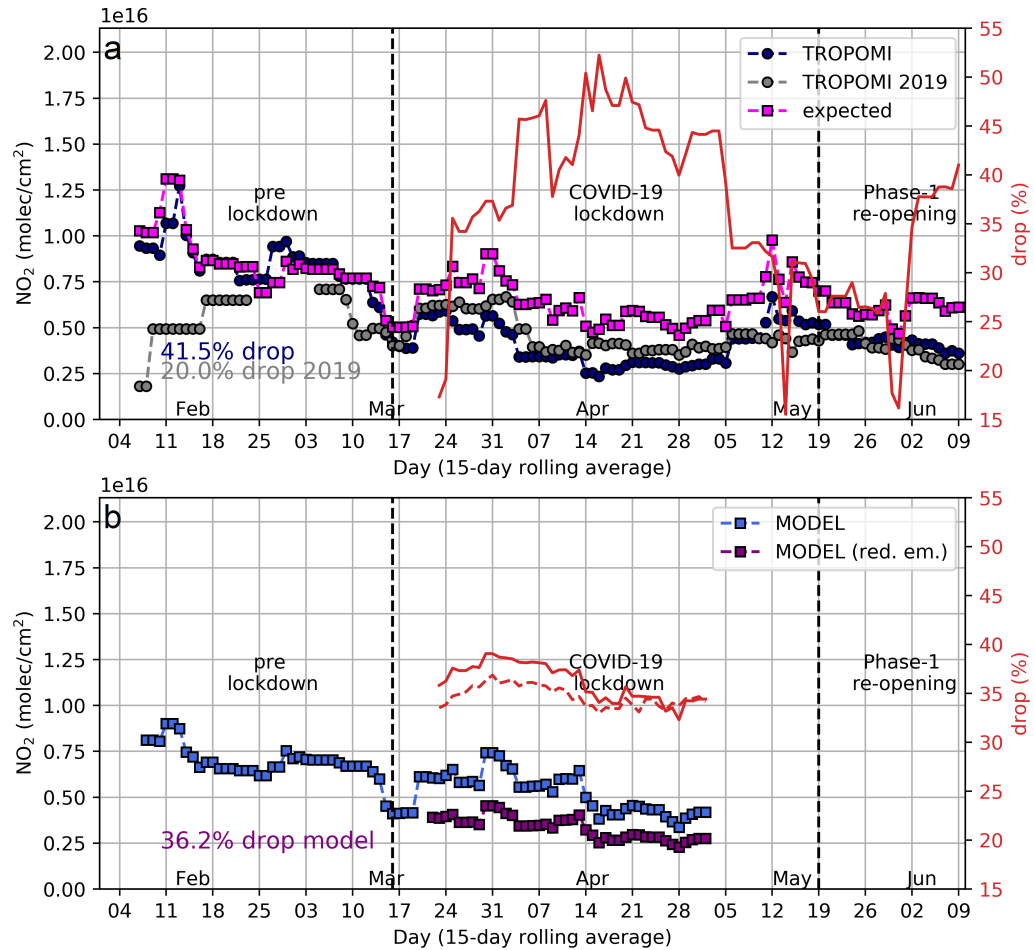


Figure 4. Timeseries of 15-day running mean of NO₂ VCDs over Toronto and Mississauga for 15 February to 9 June 2020, panel (a) shows the TROPOMI observations (navy), the expected columns (magenta). The timeseries of 2019 TROPOMI observations (grey) for the same period is shown as a reference. The red line indicates the percentage emission reductions based on the difference between the TROPOMI observations and expected columns. Panel (b) shows NO₂ columns from the model predictions sampled like TROPOMI assuming a BAU scenario with 2020 updated emissions (blue) and a 2020 COVID reduced emissions scenario (purple). The percentage decrease in model predicted VCDs (red line) is estimated from the difference between the two model runs, the red dashed line shows the drop for perfect sampling. Average emission reductions are highlighted using observations between March 16 to May 8, 2020.